Separation efficiency of a hydrodynamic separator using a 3D computational fluid dynamics multiscale approach

Vivien Schmitt, Matthieu Dufresne, Jose Vazquez, Martin Fischer and Antoine Morin

ABSTRACT

The aim of this study is to investigate the use of computational fluid dynamics (CFD) to predict the solid separation efficiency of a hydrodynamic separator. The numerical difficulty concerns the discretization of the geometry to simulate both the global behavior and the local phenomena that occur near the screen. In this context, a CFD multiscale approach was used: a global model (at the scale of the device) is used to observe the hydrodynamic behavior within the device; a local model (portion of the screen) is used to determine the local phenomena that occur near the screen. The Eulerian–Lagrangian approach was used to model the particle trajectories in both models. The global model shows the influence of the particles' characteristics on the trapping efficiency. A high density favors the sedimentation. In contrast, particles with small densities (1,040 kg/m^3) are steered by the hydrodynamic behavior and can potentially be trapped by the separator. The use of the local model allows us to observe the particle trajectories near the screen. A comparison between two types of screens (perforated plate vs expanded metal) highlights the turbulent effects created by the shape of the screen.

Key words | 3D CFD, hydrodynamic separator, multiscale approach, particle tracking, screen separation

Vivien Schmitt (corresponding author)
Matthieu Dufresne
Jose Vazquez
Martin Fischer
National School for Water and Environmental Engineering of Strasbourg (ENGEES),
ICube (University of Strasbourg, CNRS, INSA of Strasbourg, ENGEES),
Mechanics Department,
Fluid Mechanics Team,
ENGEES, 1 quai Koch, BP 61039, 67070 Strasbourg cedex,
France
E-mail: *vivien.schmitt@engees.unistra.fr*

Antoine Morin
Hydroconcept,
ZA Trappes Elancourt,
46 avenue des frères Lumière, 78190 Trappes,
France

INTRODUCTION

A significant proportion of pollutants is fixed on sediments and particles (Chebbo 1992; Chocat 1997; Ashley *et al.* 2004). In this context, the installation of special devices such as hydrodynamic separators can be a solution to protect receiving watercourses. Hydrodynamic separators are small structures currently used to capture large wastes and sediments. Several designs of hydrodynamic separator exist, each having its own operating process (Office of Water & US Environmental Protection Agency 1999). The use of a solid/liquid separation mechanism along a screen allows the last generation of such devices to increase the efficiency of hydrodynamic separators (Andoh & Saul 2003). The CycloneSep® works with these screening effects. The influent swirls and the screen retains debris and sediments on the external part of the device. After passing through the screen, the effluent is discharged to the environment. The efficiency of some hydrodynamic separators for trapping sediments has been investigated by experimental campaigns (Jefferies *et al.* 1998; Pathapati & Sansalone 2009; Schmitt *et al.* 2012). However, the mechanisms concerning the trapping efficiency of particles smaller than the aperture size of the screen is unexplored. Is it a simple sedimentation process or does the screen have an effective impact on the water/particle separation efficiency? In this context, a study with computational fluid dynamics (CFD) modeling has been performed.

The aim of this article is to use the multiscale approach developed by Schmitt *et al.* (2013) to study the efficiency of the hydrodynamic separator at the global and the local scale. The methodology of the study consists of:

- studying and comparing the hydrodynamic characteristics with the particle trajectories;
- observing the influence of the particle characteristics in the trapping efficiency;
- assessing the influence of the screen shape in the local performance.

doi: 10.2166/wst.2014.014

The long-term objective is to optimize the device and the shape of the screen and to draw conclusions about the optimal configuration.

METHODS

Multiscale CFD approach

Fluid flow modeling

CFD is a powerful tool to investigate the hydraulic behavior of hydraulic structures. It has been successfully used for storage tanks (Stovin & Saul 1994; Adamsson *et al.* 2003; Dufresne *et al.* 2009; Lipeme-Kouyi *et al.* 2010), lamella settlers (Vazquez *et al.* 2010) and hydrodynamic separators (Pathapati & Sansalone 2009; Lee *et al.* 2010). The complexity of the geometry studied here (in particular the number and the shape of the apertures of the screen) requires the use of a multiscale method (Schmitt *et al.* 2013). Therefore, two models are built (Figure 1).

Local scale model

The aim of the first model is to reproduce the hydrodynamic phenomena that occur near the screen. The volume of the geometry was reduced to a portion of a cylinder (angle of 5°, radius of 0.5 m, height of 0.04 m). The mesh was built with the 'cut-cell method' (Ansys 2013) and is composed of 2,500,000 cells. A near wall model approach was used to model the flow in the boundary layer ($y^+ \approx 1$). The turbulence RSM (Reynolds stress model) was used in order to take into account the effect of anisotropy of the turbulence on the velocity field. At boundaries, the tangential velocity measured near the screen was imposed as an inlet velocity (0.717 m/s corresponding to a discharge of 25 L/s (Schmitt *et al.* 2012)). At the outlet, a negative velocity was selected to impose the discharge passing through the screen. This simulated discharge (0.042 L/s) is calculated proportionally to the global discharge (25 L/s). The turbulence intensity (4.4%) and the hydraulic diameter (0.04 m) are also considered in the simulation. These constants calculated with Equations (1) and (2)

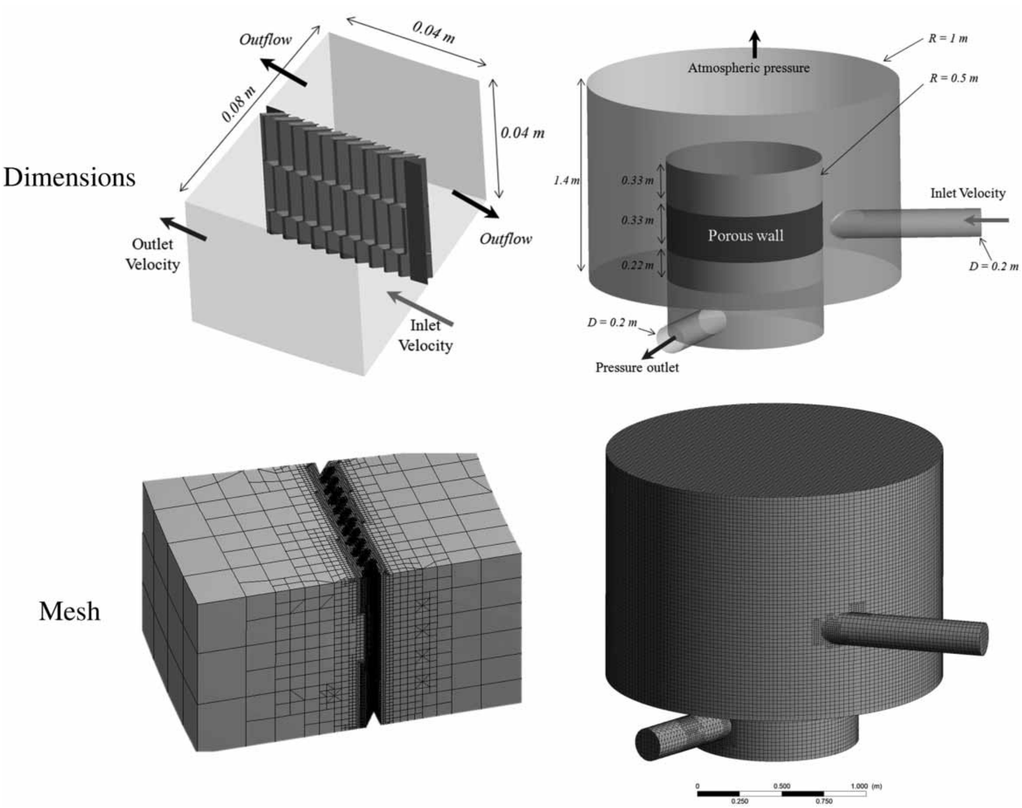

Figure 1 | Dimensions, hydraulic conditions and mesh discretization for the local scale model and for the global scale model.

are defined at the boundaries to reproduce turbulence in the model:

$$I = 0.16\mathrm{Re}^{-1/8} \quad (1)$$

$$\mathrm{Re} = \frac{UD_h}{\nu} \quad (2)$$

with I being the turbulence intensity, Re the Reynolds number, U the velocity, D_h the hydraulic diameter, ν the kinematic viscosity.

Outflow conditions are applied on the inner surface in order to evacuate the water that goes through the screen. The top and the bottom surfaces are considered as symmetry conditions. The front and the back boundaries are also considered as symmetry conditions to implement the continuity of the flow. The symmetry condition is defined by a zero normal velocity and zero normal gradients of all variables. It can be used for example to model zero-shear slip. In the present study, a symmetry condition has been used to reduce the extent of the computational domain around the grid where the velocity is almost uniform.

The energy loss created by the screen is calculated with the following equation (Pernès 2004):

$$\Delta H = \frac{\iint_{\text{Inlet}} \rho g\left(z + \frac{P}{\rho g} + \frac{V^2}{2g}\right).V_t\mathrm{d}S - \iint_{\text{Outlet}} \rho g\left(z + \frac{P}{\rho g} + \frac{V^2}{2g}\right).V_t\mathrm{d}S - \iint_{\text{OutletScreen}} \rho g\left(z + \frac{P}{\rho g} + \frac{V^2}{2g}\right).V_t\mathrm{d}S}{\rho g Q} \quad (3)$$

with ΔH the head loss, ρ the fluid density, g the gravity acceleration, z the altimetric position, P the pressure, V the velocity magnitude, V_t the tangential velocity and S the surface.

Global scale model

A conceptual screen is used at the global scale to reproduce the energy loss of the grid; the energy loss coefficient of the grid is calibrated based on the results obtained at the local scale. This method allows us to simulate the global hydrodynamic behavior of the device without needing a detailed mesh near the screen (Schmitt *et al.* 2013). This approach introduces a source term S_i that reproduces the energy loss of the screen; the model is relevant for high Reynolds numbers. This term is composed by the head loss coefficient K, the thickness of the screen Δm, the fluid density ρ and the velocity v:

$$S_i = -\left(\frac{K}{\Delta m}\frac{1}{2}\rho v^2\right) \quad (4)$$

The multiphasic 'volume of fluid' model is chosen in order to reproduce the free surface position. The RSM model was suggested for swirling flows (Ansys 2013). An inlet velocity sets the nominal discharge at 25 L/s. The turbulence intensity and the hydraulic diameter are also prescribed at the inflow boundary. A pressure condition at the outlet regulates the downstream water level. Atmospheric pressure is applied at the top of the volume. A grid sensitivity analysis allows us to choose the mesh size. The numerical uncertainty was estimated using the grid convergence index (GCI) approach (Roache 1994). Two meshes were used. A fine mesh with 2,800,000 cells and another one with 1,200,000 are compared. The GCI profiles between the two meshes were less than 1%. The model with 1,200,000 cells is sufficient to have low numerical uncertainties.

It should be noted that the calculations are executed with a HPC (high-performance computing) cluster with 48 processors and that 4.2 and 15 h are respectively necessary to obtain the converge solutions for the local scale model and the global scale model.

Particle trajectory modeling

The trapping efficiency of the device is evaluated with a Lagrangian approach. This method was used to observe the particle trajectories in sedimentation tanks, basins (Stovin & Saul 1998; Dufresne *et al.* 2009; Vosswinkel *et al.* 2012) and hydrodynamic separators (Egarr *et al.* 2004; Osei & Andoh 2008; Pathapati & Sansalone 2009).

At first, the multiscale approach is used to observe the particle trajectories in the device. Even if the global model cannot be used to determine the actual efficiency of the device (because of the simplification of the grid with a porous wall), it can be used to investigate the influence of the particle characteristics on the efficiency. The porous wall is used to reproduce the hydrodynamic behavior and cannot model the collision between the particle and the solid part of the screen. An 'interior' condition is used for the porous wall to ensure the continuity of the particle trajectory downstream of the screen. However, this model will be used to observe the influence of the particle characteristics (density and diameter) on the sedimentation process and to determine what kind of particle can potentially pass through the screen. A comparison with the hydrodynamic behavior is made to find a link with the particles' trajectories. Three diameters are studied (500, 1,000 and 1,500 μm) for various densities (1,040 to 2,600 kg/m^3). These values correspond to a range representing particles of a stormwater sewer system. The sedimentation process at the global scale is calculated by making a mass balance between the particles that are injected and the particles trapped by the separator:

$$\text{Eff}(\%) = \text{Particles retained}/\text{Particles injected} \times 100 \tag{5}$$

The local model is used to estimate qualitatively the influence of the shape of the screen. Indeed, only a portion is modeled and the screen efficiency does not correspond to the device efficiency. A comparison between two types of screens (expanded metal vs perforated plate) enables us to observe the influence of the shape on the efficiency. The visualization of the turbulence kinetic energy and the particle trajectories shows the influence of the local hydrodynamic effects. Different characteristics of particles are investigated: four diameters (35, 500, 1,200 and 1,500 μm) and four densities (1,040, 1,200, 1,700 and 2,500 kg/m^3). The screen efficiency is calculated as Equation (5).

In this approach, the particle trajectories are derived from Newton's second law and summarized by the following equations:

$$\frac{du_p}{dt} = F_D(u - u_p) + \frac{g_x(\rho_p - \rho)}{\rho_p} + F_x \tag{6}$$

with

$$F_D = \frac{18\mu}{\rho_p d_p^2}\frac{C_D R_p}{24} \tag{7}$$

$$R_p = \frac{\rho d_p |u_p - u|}{\mu} \tag{8}$$

$$C_D = a_1 + \frac{a_2}{R_p} + \frac{a_3}{R_p^2} \tag{9}$$

$$C_D = \frac{24}{R_p} \tag{10}$$

Here u_p is the particle velocity; u the fluid velocity; ρ the fluid density; ρ_p the particle density; g_x the gravity and F_x additional forces such as body forces and forces due to pressure gradients. The drag force F_D is composed of the water molecular viscosity μ, the particle diameter d_p, the Reynolds number of the particle R_p, the drag coefficient C_D. The value of C_D depends on the flow regime, and a_1, a_2 and a_3 are empirical constants. For small Reynolds number ($R_p < 0.1$), the drag coefficient is calculated with Equation (10); for $0.1 < R_p < 1{,}000$ with Equation (9); and for $R_p > 1{,}000$ it is constant and equal to 0.4. Concerning the interaction with walls, the reflect condition is imposed. The particles that hit the walls will be therefore back in the flow.

RESULTS

Global scale investigations

The validation of the multiscale method in Schmitt *et al.* (2013) allows us to use a Lagrangian approach for the global model. Figure 2 shows the influence of the particle density and the particle diameter. The device traps all particles coarser than 500 μm and 2,600 kg/m^3 for a flow rate equal to 25 L/s. By observing the graph, we can suppose that particles with low diameters and low densities are potentially steered by the hydraulic behavior: 100% of the particles lower than 1,040 kg/m^3 pass through the conceptual screen.

To explain the previous results, we have drawn the trajectories of 10 particles with various characteristics (Figure 3). A greater density is responsible for a quick sedimentation of the particle. For the case 4, particles are directly on the bed of the device and turn around the central plate. In contrast, the distribution of particles with small densities (case 1 and case 2) is mainly controlled by the mean flow. Particles are swirling around the screen approximately eight times before passing through the porous screen. This behavior is relevant for the residence time of a fluid particle (Schmitt *et al.* 2012). This confirms the fact that particles with low densities are steered by the hydrodynamic behavior.

Screen efficiency

The simulated fluid flow allows us to observe the impact of the screen shape. By increasing the angle of the metal stripe and decreasing the aperture size, the pressure and the turbulence kinetic energy gradients increase, which probably favors the ejection of particles. These phenomena are clearly illustrated in Figure 4. A zone with high turbulence

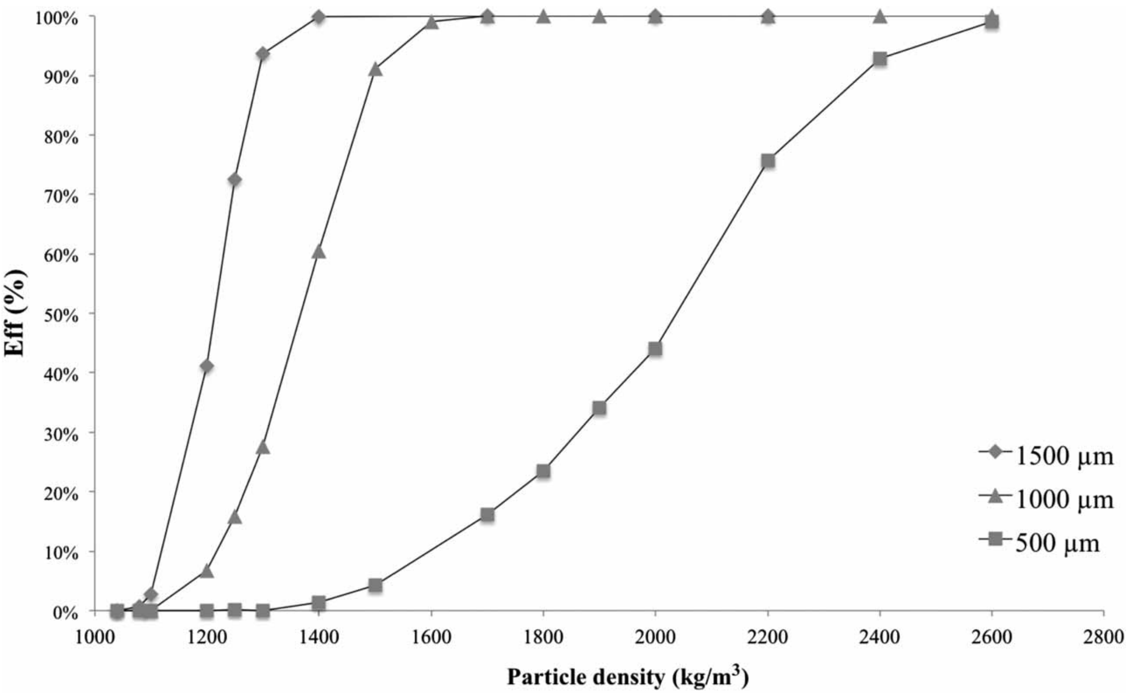

Figure 2 | Particles trapping efficiency (Eff) with the conceptual porous screen ($Q = 25$ L/s) for different particle densities and diameters.

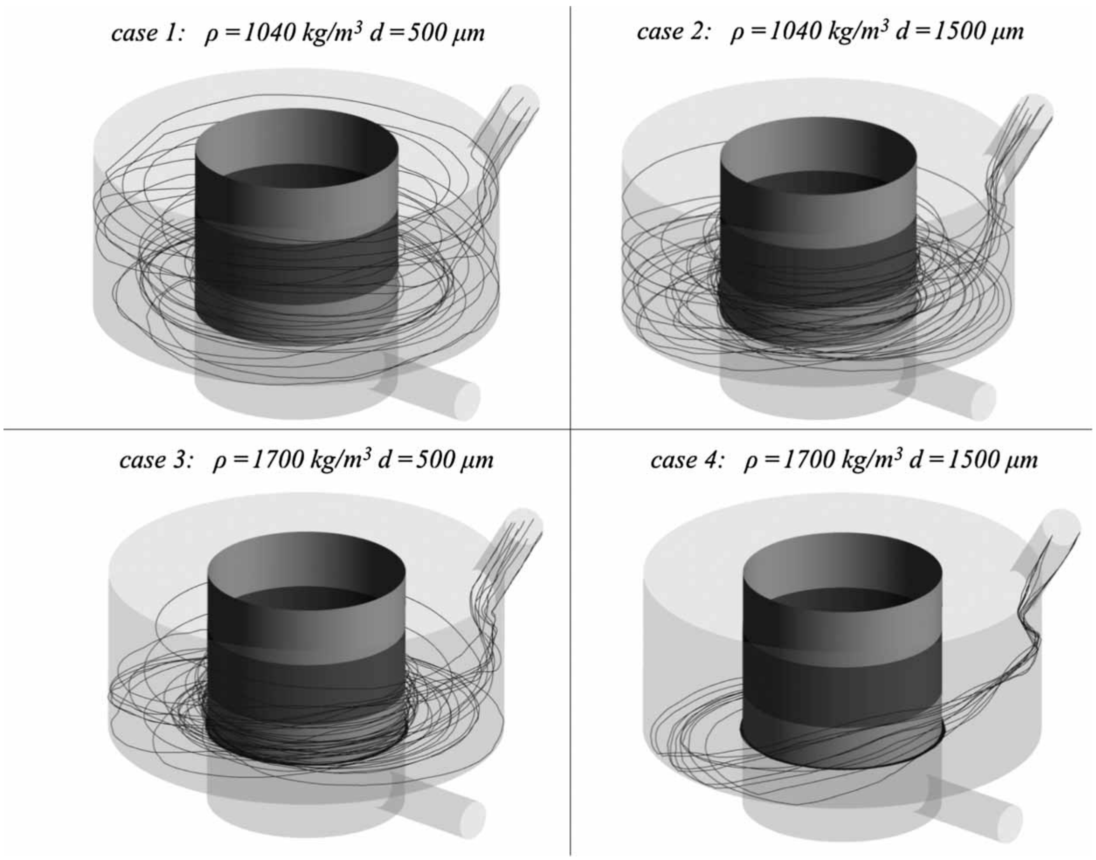

Figure 3 | Trajectories of 10 particles using the global scale model for a flow rate equal to 25 L/s.

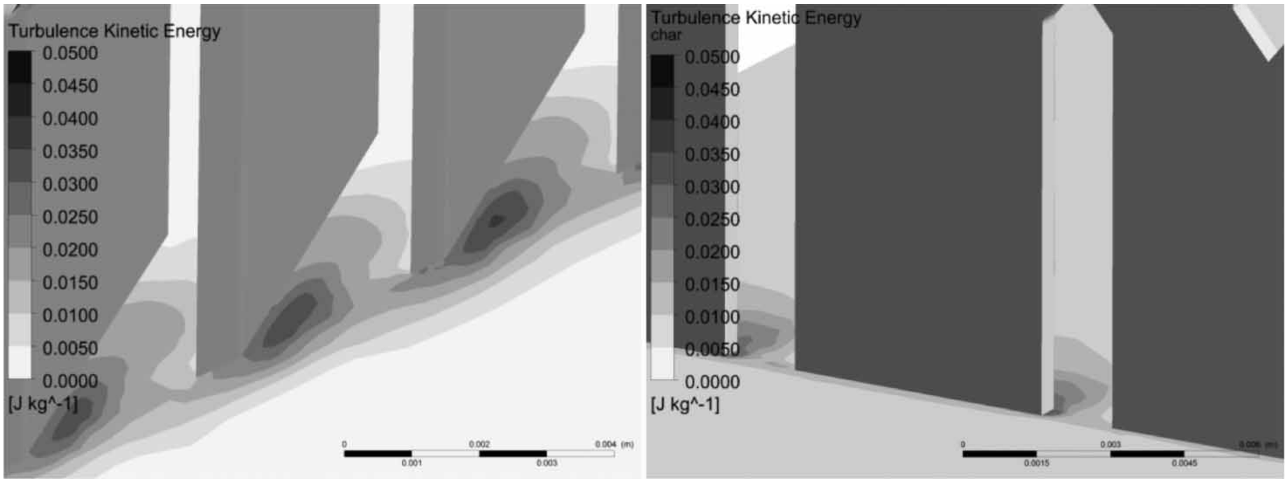

Figure 4 | Turbulence kinetic energy field for two different screens for an equivalent flow rate of 25 L/s: expanded-metal screen (left) and perforated plate with hexagonal holes (right).

Table 1 | Screen efficiency (Eff) of expanded-metal screen compared to the perforated plate

	d = **1,200 μm**			***d*** = **35 μm**		
Density	**Eff expanded metal (%)**	**Eff perforated plate (%)**	**Eff expanded metal/Eff perforated plate (%)**	**Eff expanded metal (%)**	**Eff perforated plate (%)**	**Eff expanded metal/Eff perforated plate (%)**
$\rho = 1{,}200\ \text{kg/m}^3$	86	50	172	65	46	141
$\rho = 1{,}700\ \text{kg/m}^3$	98	64	166	65	46	141
$\rho = 2{,}500\ \text{kg/m}^3$	100	71	141	65	47	138

(0.035 J/kg) is present in the opening of the expanded-metal screen. For the perforated plate, the turbulent zone is present downstream of the screen. Upstream of the screen, the turbulence kinetic energy is equal to 0.005 J/kg.

The particle tracking enables us to observe the efficiency of a screen by comparing the two screens. The results are shown in Table 1. For the same hydraulic conditions, the expanded-metal screen retains about 140% more particles than the perforated plate (column 3). The efficiency is increased for larger particles with low densities. For particles with a diameter equal to 1,200 μm and density of 1,200 kg/m^3, the expanded-metal screen retains 172% more particles than a perforated plate.

The explanation is probably the inertia of the particles. For low densities, the trajectories of the particles are easily modified. In contrast, the trajectories of heavy particles are more difficult to modify.

The link between the turbulence kinetic energy, the particle tracking and the local efficiency will be the object of a further work.

CONCLUSIONS

The objective of the study was to use a CFD multiscale approach to observe and explain the interaction between particle trajectories and the various hydrodynamic phenomena that occur in a hydrodynamic separator at different scales. The solid/liquid efficiency was predicted using a Lagrangian particle tracking at the two scales.

The global behavior showed that the trapping efficiency of the device is a function of the particle characteristics. The hydrodynamic separator traps heavy particles by sedimentation. Results obtained with the numerical method showed that the particles with small densities are steered by the hydrodynamic behavior. This kind of particle can only be retained by the local phenomena produced by the screen.

The local scale model enabled us to observe the influence of the screen shape. The comparison between two types of screens allowed us to observe the effect of the turbulence kinetic energy on the particle trajectories. A higher turbulent zone favors the ejection of particles. The inertia process can explain the fact that particles with low densities are more sensitive.

To conclude, the use of a CFD multiscale approach and particle tracking is relevant for predicting solid separation along a screen. The long-term objective is to use this methodology optimization of the device (favor the deposition, avoid the resuspension of sediments) and also the screen shape (increase the turbulence kinetic energy field and the pressure effects).

ACKNOWLEDGEMENTS

We would like to acknowledge the firm Steinhardt Wassertechnik for the construction of the pilot, Ile de France Innovation, and the GEMCEA for its financial support. We also would like to acknowledge the HPC centre of the University of Strasbourg for the computational clustering support.

REFERENCES

Adamsson, Å., Stovin, V. R. & Saul, A. J. 2003 Bed shear stress boundary condition for storage tank sedimentation. *Journal of Environmental Engineering* **129** (7), 651–658.

Andoh, R. Y. G. & Saul, A. J. 2003 The use of hydrodynamic vortex separators and screening systems to improve water quality. *Water Science and Technology* **47** (4), 175–183.

Ansys 2013 *Fluent 14.0 User's Guide*. Ansys Inc., Canonsburg, PA, USA.

Ashley, R. M., Bertrand-Krajewski, J. L. & Hvited-Jacobsen, T. 2004 *Solids in Sewers*. Scientific and Technical Report no. 14, IWA Publishing, London.

Chebbo, G. 1992 *Solides des rejets urbains par temps de pluie: caractérisation et traitabilité (Particles in urban runoffs during rainfall events, characterization and variability)*. PhD thesis, Ecole nationale des ponts et chaussées, Paris, France.

Chocat, B. 1997 Encyclopédie de l'hydrologie urbaine et de l'assainissement, Bassins de retenue p. 95, Eurydice 92, Ed Tec&Doc Lavoisier, Paris, 1997, 1121 pp.

Dufresne, M., Vazquez, J., Terfous, A., Ghenaim, A. & Poulet, J. B. 2009 Experimental investigation and CFD modelling of flow, sedimentation, and solids separation in a combined sewer detention tank. *Computers & Fluids* **38** (5), 1042–1049.

Egarr, D. A., Faram, M. G., O'Doherty, T. & Syred, N. 2004 An investigation into factors that determine the efficiency of a hydrodynamic vortex separator. In: *5th International Conference on Innovative Technologies in Urban Storm Drainage*, Novatech'04, Lyon, France.

Jefferies, C., Allinson, C. L. & McKeown, J. 1998 The performance of a novel combined sewer overflow with perforated conical screen. *Water Science and Technology* **37** (1), 243–250.

Lee, J. H., Bang, K. W., Choi, C. S. & Lim, H. S. 2010 CFD modelling of flow field and particle tracking in a hydrodynamic stormwater separator. *Water Science and Technology* **62** (10), 2381–2388.

Lipeme-Kouyi, G., Arias, L., Barraud, S. & Bertrand-Krajewski, J.-L. 2010 CFD Modelling of flow in a large stormwater detention and settling basin. In: *Seventh International Conference on Innovative Technologies in Urban Storm Drainage*, Novatech'10, Lyon, France.

Office of Water and US Environmental Protection Agency 1999 Stormwater Technology Fact Sheet: Hydrodynamic Separator. US Environmental Protection Agency, Washington, DC.

Osei, K. & Andoh, R. 2008 Optimal grit and control in collection systems and at treatment plants. In: *World Environmental & Water Resources Congress*. May 12–16, 2008, Honolulu, Hawaii.

Pernès, P. 2004 *Hydraulique Unidimensionnelle: Partie 1 et 2 (Unidimensional Hydraulics, Part 1 and 2)*. Cemagref editions.

Pathapati, S. S. & Sansalone, J. J. 2009 CFD modeling of a stormwater hydrodynamic separator. *Journal of Environmental Engineering* **135** (4), 191–202.

Roache, P. J. 1994 Perspective: a method for uniform reporting of grid refinement studies. *Journal of Fluids Engineering* **116**, 405–413.

Schmitt, V., Dufresne, M., Vazquez, J., Fischer, M. & Morin, A. 2012 *Etude Expérimentale et Numérique du CycloneSep. Rapport de Convention d'Étude pour la Société Hydroconcept (Experimental and CFD Study of the CycloneSep. Final Report for Hydroconcept)*. ENGEES, Strasburg, Germany.

Schmitt, V., Dufresne, M., Vazquez, J., Fischer, M. & Morin, A. 2013 Optimization of a hydrodynamic separator using a multiscale computational fluid dynamics approach. *Water Science and Technology* **68** (7), 1574–1581.

Stovin, V. R. & Saul, A. J. 1994 Sedimentation in storage tank structures. *Water Science and Technology* **29** (1–2), 363–372.

Stovin, V. R. & Saul, A. J. 1998 A computational fluid dynamics (CFD) particle tracking approach to efficiency prediction. *Water Science and Technology* **37** (1), 285–293.

Vazquez, J., Morin, A., Dufresne, M. & Wertel, J. 2010 Optimisation de la forme des décanteurs lamellaires par la modélisation hydrodynamique 3D (A CFD approach for shape optimization of lamellar settlers). In: *Seventh International Conference on Innovative Technologies in Urban Storm Drainage*, Novatech'10, Lyon, France.

Vosswinkel, N., Schnieders, A., Maus, C., Ebbert, S., Mohn, R. & Uhl, M. 2012 Comparison of flow and sedimentation pattern for three designs of storm water tanks by numerical modelling (CFD). In: *9th International Conference on Urban Drainage Modelling*, Belgrade, Serbia.

First received 24 July 2013; accepted in revised form 3 January 2014. Available online 17 January 2014